


A single supratentorial high-grade neuroepithelial tumor with two distinct *BCOR* mutations, exceptionally long complete remission and survival

Juliane Bremer^{1,2}  | Raimund Kottke³ | Pascal D. Johann^{4,5,6} | Katja von Hoff⁷ | Pierluigi Brazzola⁸ | Michael A. Grotzer⁹ | Marcel Kool^{4,5,10} | Elisabeth Rushing¹ | Nicolas U. Gerber⁹

¹Institute of Neuropathology University Hospital Zurich, Zurich, Switzerland

²Institute of Neuropathology University Hospital RWTH Aachen, Aachen, Germany

³Department of Diagnostic Imaging, University Children's Hospital Zurich, Zurich, Switzerland

⁴Hopp Children's Cancer Center (KITZ), Heidelberg, Germany

⁵Division of Pediatric Neurooncology, German Cancer Research Center (DKFZ) and German Cancer Consortium (DKTK), Heidelberg, Germany

⁶Department of Pediatric Hematology and Oncology, University Hospital Heidelberg, Heidelberg, Germany

⁷Department of Pediatric Hematology and Oncology, Charité University Medicine, Berlin, Germany

⁸Istituto Pediatrico della Svizzera Italiana, Bellinzona, Switzerland

⁹Department of Oncology, University Children's Hospital Zurich, Zurich, Switzerland

¹⁰Princess Máxima Center for Pediatric Oncology, Utrecht, The Netherlands

Correspondence

Juliane Bremer, Institute of Neuropathology, University Hospital RWTH Aachen, Pauwelsstrasse 30, 52074 Aachen, Germany.
Email: jbremer@ukaachen.de

Correction added on 11 July 2020, after first online publication: Projekt Deal funding statement has been added.

Funding information

Universität Zürich, Grant/Award Number: Filling the Gap career development program

Abstract

Here, we present a patient with high-grade neuroepithelial tumors with mutations in the BCL6 corepressor *BCOR* (HGNET-*BCOR*), a rare, highly malignant brain tumor with poor prognosis. The patient underwent gross total tumor resection (GTR), high-dose chemotherapy, and, after local relapse, GTR, proton radiation, and chemotherapy. After a 7.5 year-long complete remission, the tumor recurred locally, was treated by GTR, and responded to temozolomide treatment. In addition to an internal tandem duplication in *BCOR* common to the majority of HGNET-*BCOR* cases, molecular analysis revealed a second *BCOR* mutation in this tumor: a frame shift mutation. The combination of these mutations was associated with relatively low *BCOR* expression compared to other HGNET-*BCOR* cases.

KEYWORDS

BCOR, brain tumor, HGNET-*BCOR*, high-grade neuroepithelial tumor

Abbreviations: AA, amino acids; ASCT, autologous stem cell transplantation; *BCOR*, BCL6 corepressor; CCNU, chloroethyl-cyclohexyl-nitrosourea; CNS-PNET, central nervous system primitive neuroectodermal tumor; DWI, diffusion-weighted imaging; GTR, gross-total tumor resection; HDCT, high-dose chemotherapy; HGNET-*BCOR*, high-grade neuroepithelial tumors with mutations in the BCL6 corepressor *BCOR*; ITD, internal tandem duplication; SHH, sonic hedgehog; WGS, whole genome sequencing.

This is an open access article under the terms of the Creative Commons Attribution-NonCommercial-NoDerivs License, which permits use and distribution in any medium, provided the original work is properly cited, the use is non-commercial and no modifications or adaptations are made.

© 2020 The Authors. *Pediatric Blood & Cancer* published by Wiley Periodicals LLC

1 | INTRODUCTION

Based on recent advances in molecular neuropathology, a majority of tumors previously designated as central nervous system primitive neuroectodermal tumors (CNS-PNET) have been reclassified as other known tumor entities, for example, high-grade gliomas. In addition, several new molecularly distinct entities were discovered among these CNS-PNETs, which were subsequently also identified in other tumor cohorts with different histologies, such as ependymomas or glioblastomas. One of these newly identified molecularly distinct brain tumor entities is the high-grade neuroepithelial tumor with mutation in the BCL6 corepressor *BCOR* (HGNET-BCOR).¹ HGNET-BCOR is rare, affects young children, can arise in any location in the CNS, and available data suggest a poor prognosis.¹ To date, there is no standard of care therapy for HGNET-BCOR patients. The majority of reported cases have been treated with surgery, irradiation, and combination chemotherapy. To our knowledge, there is only one previously reported case with survival of 5 years beyond initial diagnosis,² but since this is a novel entity, the follow up for most reported cases is short.

2 | RESULTS

A previously healthy 2-year-old female child presented for evaluation after 4 weeks of persistent nausea and vomiting with acute clinical deterioration. Physical examination revealed anisocoria, and magnetic resonance imaging (MRI) of the head revealed a large, well-demarcated bifrontal mass accompanied by enlarged lateral ventricles due to compression of the third ventricle (Figure 1A,B). The patient was admitted to the neurosurgical unit and underwent gross-total tumor resection (GTR). Postoperatively, the patient suffered temporary left-sided facial and arm paresis as well as transient epileptic seizures. Neuropathological examination of the biopsy showed a relatively sharply demarcated tumor with extensive large and small necrotic foci with pseudopalisading tumor cells, focal microvascular proliferation, numerous apoptotic bodies and mitoses, and an arborizing capillary network with occasional anuclear perivascular zones (Figure 1I). GFAP was focally expressed (Figure 1J). At the time of initial diagnosis, no definitive neuropathological diagnosis was rendered. Differential diagnoses included CNS-PNET with focal glial differentiation and small cell glioblastoma.

Based on the initial differential diagnosis of a CNS-PNET, the patient was treated within the HIT 2000 trial of the Society for Paediatric Oncology and Haematology (GPOH) with three cycles carboplatin + etoposide + intraventricular methotrexate followed by tandem high-dose chemotherapy (HDCT; carboplatin + etoposide/thiotepa + cyclophosphamide, including intraventricular methotrexate), followed by autologous stem cell transplantation (ASCT).³ A first local relapse was diagnosed 17 months after diagnosis and GTR was achieved (Figure 1C,D). Neuropathological examination of the relapse showed morphological features similar to the initial tumor sample. The patient underwent craniospinal proton radiotherapy with 35.2 Gy and a boost to the tumor bed to 55 Gy,

followed by four cycles of maintenance chemotherapy with cisplatin, chloroethyl-cyclohexyl-nitrosourea (CCNU), and vincristine. The patient subsequently remained in complete remission for more than 6 years. During this period, especially during the first year after diagnosis, the patient suffered from several complications. These included subdural hemorrhage and subsequent hydrocephalus, which were managed surgically, including implantation of a peritoneal shunt, as well as shunt infection and meningitis. Approximately 9 years after initial diagnosis and 6 years after the end of treatment, the tumor recurred a second time at another site of the tumor bed (Figure 1E), and GTR was achieved. A third local relapse at still another site of the tumor bed was seen on MRI 3 months later, and oral temozolomide was administered for another 2 months (5 days on/23 days off; first cycle: 150 mg/m²/day, subsequent cycles: 200 mg/m²/day; Figure 1F). Partial response followed by stable disease was seen for more than 1 year (Figure 1G), after which a progression of the lesion (fourth progression) was diagnosed (Figure 1H) and treated with GTR. Three months later, a new, small nodular relapse (fifth progression) was discovered radiologically and confirmed on a follow-up MRI. Further local therapy is being scheduled at the time of publication of this report. Despite undergoing multiple treatments of local relapses and despite neuropsychological impairment leading to special schooling, the child is still maintaining a good quality of life.

Three biopsies of the current case (primary tumor, first, and second progression) were reevaluated by DNA methylation profiling and classified as a HGNET-BCOR tumor according to the Heidelberg classifier (www.molecularneuropathology.org).⁴ Indeed, *t*-distributed stochastic neighbor embedding (*t*-SNE) clustering analyses of the DNA profiles of this particular case with reference cases of several other pediatric brain tumor entities showed that the tumor clustered with other HGNET-BCOR cases (Figure 2A). In addition, whole genome sequencing (WGS) of tumor and germline DNA revealed a tumor specific internal tandem duplication (ITD) in exon 15 of the *BCOR* gene on chromosome X (X:39,911,418-39,911,531), confirming the diagnosis of HGNET-BCOR. In addition to the ITD, WGS revealed a second *BCOR* mutation, which is predicted to cause a frame shift mutation after 209 of 1721 amino acids (AA). Additional functional single nucleotide variants (Figure 2B) and functional insertions or deletions (Figure 2C) were detected by WGS. Transcriptomes of the primary tumor and the second relapse were analyzed to detect molecular drug targets. Marked *FGF3* overexpression was observed compared to other tumor entities (Figure 2D). *GLI1*, which is elevated upon activation of the sonic hedgehog (SHH) pathway, was increased to levels similar to medulloblastomas with activation of SHH pathway (Figure 2E), in line with previous reports of SHH pathway activation in HGNET-BCOR.^{1,5,6} Nevertheless, no suitable molecular drug target was identified based on the expression profile. Microscopically, the second tumor relapse differed from the first two biopsies. The tumor was less cellular, showed a biphasic pattern with collagen- and capillary-rich anuclear zones, and necrosis was absent (Figure 1K). *BCOR* was strongly expressed (Figure 1L). Molecularly, the tumor still exhibited the *BCOR* ITD mutation, while the *BCOR* frame shift mutation was no longer detectable (Figure 2C). Interestingly, *BCOR* mRNA expression levels were lower

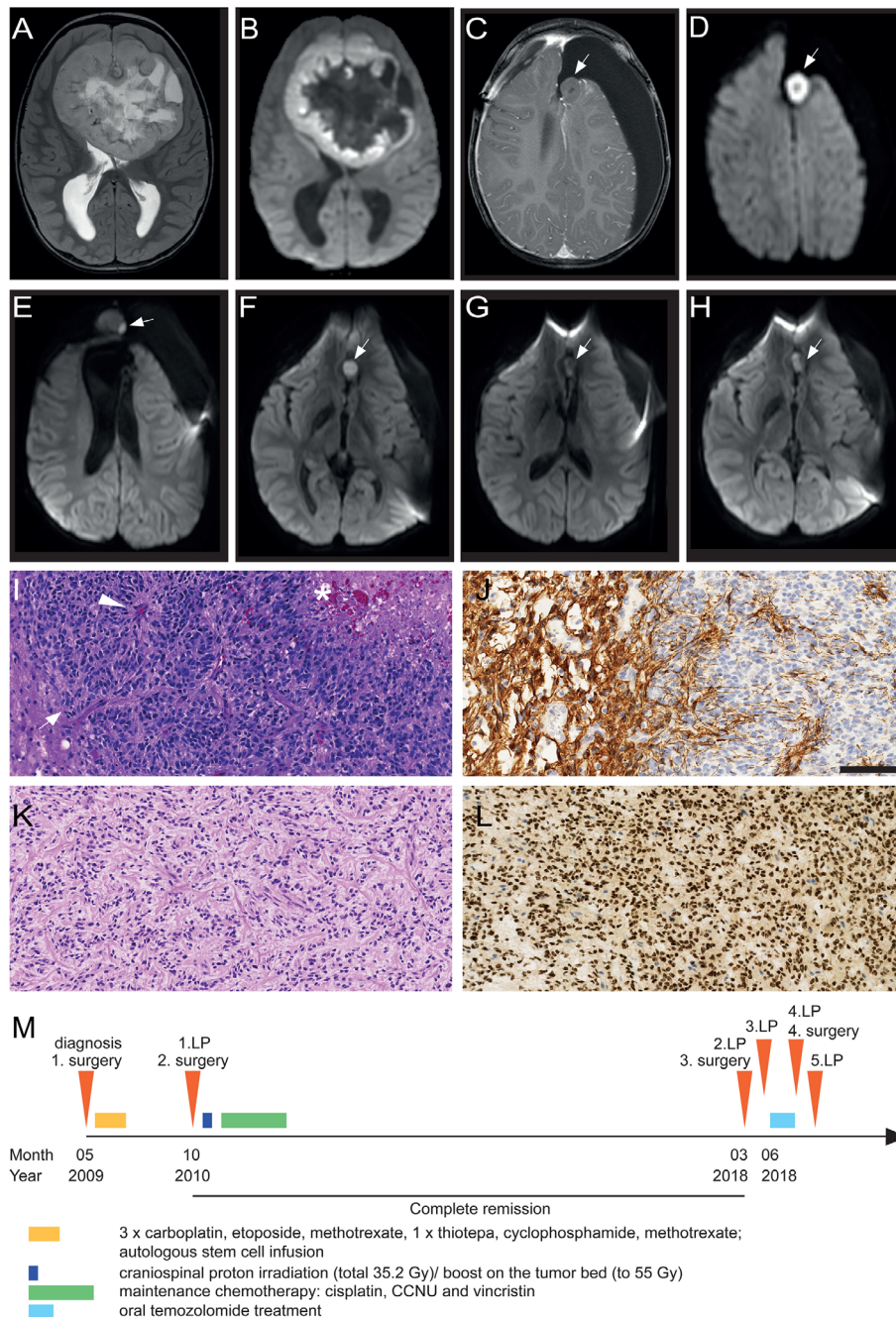


FIGURE 1 Radiological and pathological tumor assessment. A-H, Radiological tumor assessment by MRI. MRI of the primary tumor with axial T2-weighted image showing a well-demarcated mass with central hyperintense areas suggestive of cystic-necrotic changes, absence of peritumoral edema, and enlarged lateral ventricles due to compression of the third ventricle (A). Peripheral restricted diffusion in the tumor on diffusion-weighted imaging (DWI) trace image indicating high cellularity (B). Axial T1-weighted image of the first local relapse demonstrating nonenhancing parasagittal nodule (C) with diffusion restriction (D). DWI trace image of the second local relapse showing a small anterior parasagittal nodule with restricted diffusion (E). F-H, DWI trace images of the third local relapse (F, August 2018, MRI before temozolomide treatment), response to temozolomide (G, May 2019), and fourth local progression (H, August 2019). Tumor is marked by arrows in (C-H). I-L, Microscopic pathology. HE-stained section of the primary tumor (I) showing a relatively sharply demarcated highly cellular tumor composed of uniform small spindle to ovoid tumor cells with scant fibrillary cytoplasm. Sharp demarcation is marked by a white arrow. Tumor vessels displayed an arborizing capillary network with occasional anuclear perivascular zones (white arrowhead), frequent pseudopalisading necrosis (white star), and numerous apoptotic bodies and mitoses were seen. Immunohistochemistry of the primary tumor showed focal GFAP expression (J), with the majority of the tumor being GFAP negative. Synaptophysin and neurofilament proteins were not expressed by the tumor and nuclear INI1 expression was retained. The MIB1 proliferation index reached approximately 40%. HE-stained section of the second local relapse (K), showing a less cellular tumor with a biphasic, rhythmic pattern with collagen- and capillary-rich anuclear zones. Immunohistochemistry revealed strong nuclear BCOR expression (L). M, Timeline of the tumor progression and treatment choices is shown. LP, local progression

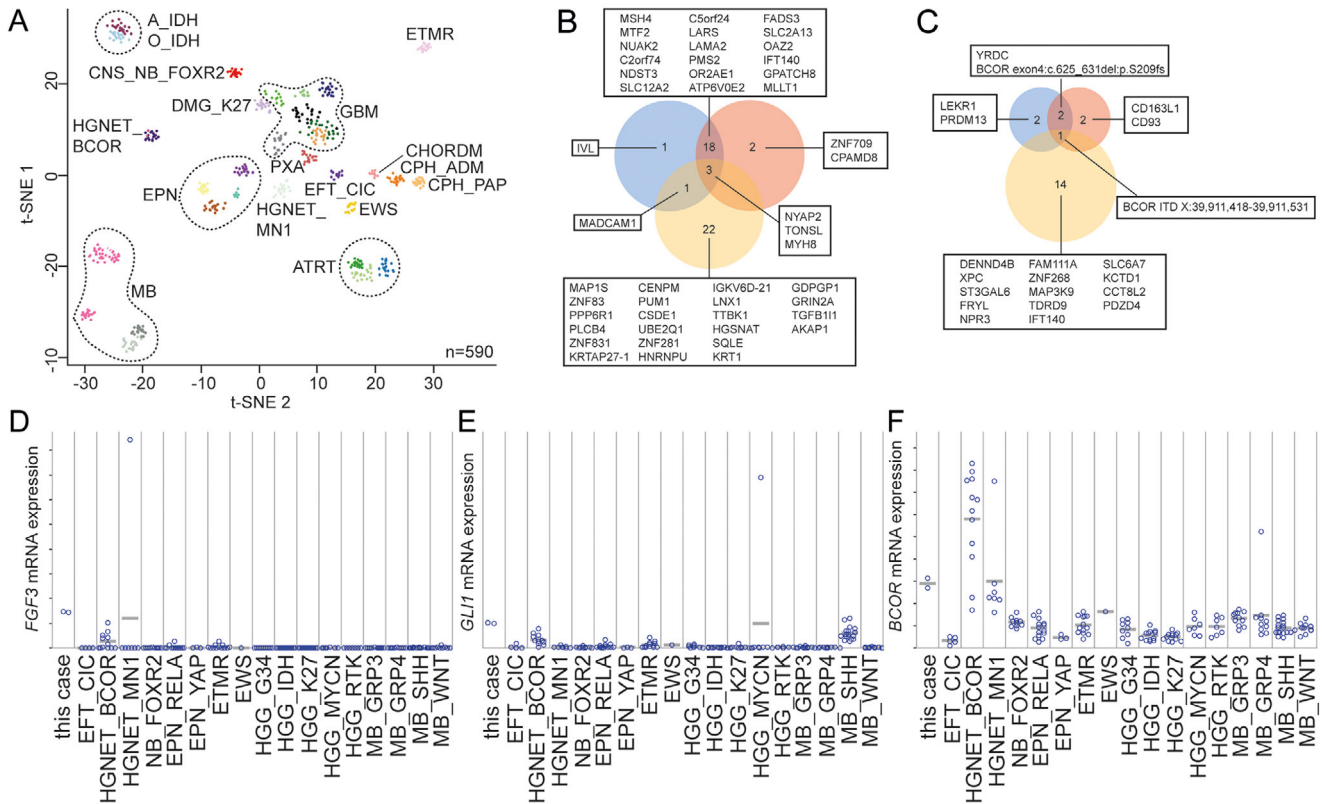


FIGURE 2 Molecular analysis of HGNET-BCOR. A, Methylation-based *t*-distributed stochastic neighbor embedding (*t*-SNE) distribution of selected central nervous system (CNS) tumor methylation classes of a reference cohort and three tumor biopsies of the case presented here (primary tumor, first and second progression of this case, total 590 samples). Reference cohort includes astrocytomas and oligodendrogliomas with IDH mutation (A_IDH, O_IDH), embryonal tumor with multilayered rosettes (ETMR), CNS neuroblastoma with FOXR2 activation (CNS_NB_FOXR2), diffuse midline glioma, H3 K27M mutated (DMG_K27), different molecular groups of glioblastoma (GBM), high-grade neuroepithelial tumor with BCOR alteration (HGNET_BCOR), pleomorphic xanthoastrocytoma (PXA), different molecular groups of ependymoma (EPN), chordoid meningioma (CHORDM), adamantinomatous (CPH_ADM) and papillary craniopharyngioma (CPH_PAP), CNS Ewing sarcoma family tumor with CIC alteration (EFT_CIC), CNS high-grade neuroepithelial tumor with MN1 alteration (CNS HGNET_MN1), Ewing sarcoma (EWS), atypical teratoid rhabdoid tumor (ATRT), and different molecular groups of medulloblastoma (MB). The three biopsies of this patient are shown in pink within the HGNET_BCOR cluster. B-C, Venn diagrams of functional single nucleotide variants (B) and functional insertions or deletions (C) identified by whole genome sequencing (WGS). Genes mutated in primary tumor (blue), first progression (red), and second progression (yellow) are shown in boxes. Mutations occurring in two or all three biopsies are also shown. D-F, *FGF3*, *GLI1*, and *BCOR* mRNA expression levels were determined by microarray analysis. Expression in this case of HGNET-BCOR (primary tumor and second progression) was compared to other cases of HGNET-BCOR and to other tumor entities, including entities listed in (A), HGG (high-grade gliomas) with G34 or K27 mutations of histone genes, IDH1 or IDH2 mutations (_IDH), mutations in *MYCN* or in genes encoding receptor tyrosine kinases (_RTK); EPN with *RELA* fusion (_RELA) or *YAP1* fusion (_YAP) and MB of the four different molecular groups: group 3, group 4, with sonic hedgehog (SHH) activation, and WNT activation (_GRP3, _GRP4, _SHH, and _WNT)

than in most other HGNET-BCOR (10/12 samples). Nuclear beta-catenin staining, which has been described in 11 of 14 HGNET-BCOR cases and considered indicative of WNT activation,¹ was not observed.

3 | DISCUSSION

Here, we present a case of HGNET-BCOR with two distinct BCOR mutations, an ITD and a frame shift mutation. In addition to surgical resection, our patient was treated with a combination of intravenous chemotherapy (including HDCT with ASCT) and intraventricular chemotherapy, and after the first local relapse with proton radiotherapy. This combination led to a sustained complete remission for

7.5 years and the patient is alive more than 10 years after initial diagnosis. Remission and survival are much longer than of most previously reported cases (Table S1).^{1-2,5-11} However, since this is a novel entity, the follow up for most of these cases is short. A further local tumor relapse was temporarily controlled by temozolomide alone. While in this case multimodal treatment contributed to long-term tumor control after relapse, future studies are required to determine which treatment optimally controls HGNET-BCOR after relapse.

The primary tumor and first recurrence exhibited two distinct BCOR mutations, an N-terminal BCOR frame shift mutation as well as the classic ITD mutation most frequently reported in HGNET-BCOR. Exon 15 ITD is known to cause overexpression of functional BCOR protein.^{6,12} Previously, BCOR inactivating mutations have been identified in

hematological malignancies, and therefore, *BCOR* has been recognized as a tumor suppressor.¹³ These findings suggest that too high and too low *BCOR* expression promotes tumorigenesis. In the case described here, while the ITD was detectable also in the second tumor progression, the frame shift mutation was no longer detectable, suggesting that the allele with the frame shift mutation was deleted during tumor evolution. Since the frame shift mutation is predicted to abrogate *BCOR* after 209 of 1721 AA, *BCOR* would lack essential domains including the PUF domain. Hence, this mutation is predicted to render *BCOR* nonfunctional. Future studies involving additional patients may indicate if a second inactivating mutation accompanying the ITD, as identified in this case, reduces the abnormally high *BCOR* expression caused by the ITD, thereby affecting outcome.

CONFLICT OF INTEREST

The authors declare that there is no conflict of interest.

ACKNOWLEDGMENTS

We would like to thank the technicians at the Institute of Neuropathology, University Hospital of Zürich for preparing the histological sections and immunohistochemistry. Juliane Bremer was funded by the Filling the Gap career development program by the University of Zürich.

Open access funding enabled and organized by Projekt DEAL.

ORCID

Juliane Bremer  <https://orcid.org/0000-0002-0268-9425>

REFERENCES

1. Sturm D, Orr BA, Toprak UH, et al. New brain tumor entities emerge from molecular classification of CNS-PNETs. *Cell*. 2016;164(5):1060-1072.
2. Ferris SP, Velazquez Vega J, Aboian M, et al. High-grade neuroepithelial tumor with *BCOR* exon 15 internal tandem duplication—a comprehensive clinical, radiographic, pathologic, and genomic analysis. *Brain Pathol*. 2019;30(1):46-62.
3. Friedrich C, von Bueren AO, von Hoff K, et al. Treatment of young children with CNS-primitive neuroectodermal tumors/pineoblastomas in the prospective multicenter trial HIT 2000 using different chemotherapy regimens and radiotherapy. *Neuro Oncol*. 2013;15(2):224-234.

4. Capper D, Jones DTW, Sill M, et al. DNA methylation-based classification of central nervous system tumours. *Nature*. 2018;555(7697):469-474.
5. Paret C, Russo A, Otto H, et al. Personalized therapy: CNS HGNET-*BCOR* responsiveness to arsenic trioxide combined with radiotherapy. *Oncotarget*. 2017;8(69):114210-114225.
6. Paret C, Theruvath J, Russo A, et al. Activation of the basal cell carcinoma pathway in a patient with CNS HGNET-*BCOR* diagnosis: consequences for personalized targeted therapy. *Oncotarget*. 2016;7(50):83378-83391.
7. Appay R, Macagno N, Padovani L, et al. HGNET-*BCOR* tumors of the cerebellum: clinicopathologic and molecular characterization of 3 cases. *Am J Surg Pathol*. 2017;41(9):1254-1260.
8. Yoshida Y, Nobusawa S, Nakata S, et al. CNS high-grade neuroepithelial tumor with *BCOR* internal tandem duplication: a comparison with its counterparts in the kidney and soft tissue. *Brain Pathol*. 2018;28(5):710-720.
9. Kirkman MA, Pickles JC, Fairchild AR, et al. Early wound site seeding in a patient with central nervous system high-grade neuroepithelial tumor with *BCOR* alteration. *World Neurosurg*. 2018;116:279-284.
10. Al-Battashi A, Al Hajri Z, Perry A, Al-Kindi H, Al-Ghaithi I. A cerebellar high-grade neuroepithelial tumour with *BCOR* alteration in a five-year-old child: a case report. *Sultan Qaboos Univ Med J*. 2019;19(2):e153-e156.
11. Haberler C, Reiniger L, Rajnai H, et al. Case of the month 1-2019: CNS high-grade neuroepithelial tumor with *BCOR* alteration. *Clin Neuropathol*. 2019;38(1):4-7.
12. Roy A, Kumar V, Zorman B, et al. Recurrent internal tandem duplications of *BCOR* in clear cell sarcoma of the kidney. *Nat Commun*. 2015;6:8891.
13. Tanaka T, Nakajima-Takagi Y, Aoyama K, et al. Internal deletion of *BCOR* reveals a tumor suppressor function for *BCOR* in T lymphocyte malignancies. *J Exp Med*. 2017;214(10):2901-2913.

SUPPORTING INFORMATION

Additional supporting information may be found online in the Supporting Information section at the end of the article.

How to cite this article: Bremer J, Kottke R, Johann PD, et al. A single supratentorial high-grade neuroepithelial tumor with two distinct *BCOR* mutations, exceptionally long complete remission and survival. *Pediatr Blood Cancer*. 2020;67:e28384. <https://doi.org/10.1002/pbc.28384>